Mechanical and Vibration Characteristics of Laminated Composite Plates Embedding Shape Memory Alloy Superelastic Wires

Silvio Pappadà, Per Gren, Kourosh Tatar, Tord Gustafson, Rocco Rametta, Ettore Rossini, and Alfonso Maffezzoli

Currently, there is a great interest in the study of shape memory alloy (SMA) composites, since SMA wires with a small diameter have become commercially available. Many potential uses have been found for SMA composites in shape control, vibration control, and for the realization of structures with improved damage tolerance. In this work, two types of SMA-hybridized composites are presented for investigating the mechanical and vibration characteristics. The first one contains unidirectional superelastic SMA wires, while the other has been realized with embedded knitted SMA layers. The samples from these laminates have been tested according to "Charpy method" (ASTM D256) and static flexural test method (ASTM D790) to evaluate the influence of the integration of thin superelastic SMA wires on the impact behavior and the mechanical properties of the hybrid composites. Moreover, since the SMA wires are expected to give damping capacity, by measuring the vibration mode of a clamped cantilever using laser vibrometry, the influence of both SMA arrangements on the vibration characteristics has been investigated. Finally, further tests have been carried out on composite panels realized by embedding unidirectional steel wires to distinguish the influence of the martensitic transformation from the pure introduction of a metallic wire into the polymeric matrix.

1. Introduction

Composite materials are commonly used in fields in which high performances, such as high resistance to different types of loads and lightweight, are requested. In many cases, these materials have to resist to static and fatigue loads or to random impacts which can occur during their lifetime. For these reasons, it is fundamental to improve the resistance behavior of composite structures, without increasing their weights and compromising other mechanical properties.

Silvio Pappadà and **Rocco Rametta**, Departments of Materials and Structures Engineering, Technologies and Processes Area, Consorzio CETMA, Cittadella della Ricerca, SS7-Km706+300, 72100 Brindisi, Italy; **Per Gren** and **Kourosh Tatar**, Division of Experimental Mechanics, Lulea University of Technology, SE-97187, Luleå, Sweden; **Tord Gustafson**, APC Composite, Karlsviksvagen 81, S-97594 Luleå, Sweden; **Ettore Rossini**, Extreme Materials S.r.l., Via dei Cipressi 2, Costa Masnaga, LC, Italy; and **Alfonso Maffezzoli**, Department of Engineering for Innovation, University of Salento, Via per Monteroni, Edificio "La Stecca", 73100 Lecce, Italy. Contact e-mails: silvio.pappada@cetma.it, rocco.rametta@cetma.it, ettore_rossini@virgilio.it, and alfonso.maffezzoli@unile.it.

In these years, there is an increasing interest on hybrid composite materials in which shape memory alloy (SMA) wires are embedded with the aim to increase their static and dynamic properties or for vibration and shape control (Ref 1-10). In fact, SMA materials, presenting unique mechanical and thermodynamic properties such as shape memory effect and pseudoelasticity, are being used as "smart" materials embedded into conventional resins or composites to obtain tunable properties and shapes, damping capacity, and self-healing capabilities. Moreover, SMA wires have been obtained with very small diameters (down to 20 to 30 µm diameter), and hybrid textile with SMA wires have been realized and used as reinforcements of hybrid composite materials for different applications. For example, SMA wires or yarns can be used as "smart fibers" combined with conventional glass/carbon fibers to realize new hybrid textile preforms, even if the fabrication process of these SMA-based preforms is still complicate and nonstandardized.

In this study, the possibility of realizing new hybrid composite with enhanced damping properties has been investigated by means of laser vibrometry (Ref 7-10). The primary advantage of using a laser vibrometer is the noncontact nature of the transducer, which eliminates mass loading of structure due to response measurements transducer. It is well known that there are two types of damping: material damping and system damping. Material damping is the damping inherent in the material, while system or structural damping includes the damping at the supports, boundaries, joints, interface, etc. Since utilizing damping materials is the most common way to reduce resonance responses, accurate measurements of damping are crucial to proper design, optimization, and modeling of systems from a vibration reduction standpoint.

Three types of hybrid composites have been realized:

– A glass-reinforced composite plate with a vinylester matrix containing unidirectional superelastic wires;
– Composite plates embedding steel wires of the same diameter of the SMA ones to discriminate the influence of the martensitic transformation of SMA from the simple introduction of metallic wires into the polymeric matrix; and
– Hybrid composites by means of glass hybrid preforms (HEP), in which SMA wires are knitted together with glass bundles to evaluate the possibility of enhancing the damping effect of superelastic wires by introducing predeformed regions into the wires.

By measuring the vibration mode of a clamped cantilever, the influences of both SMA arrangements on the vibration characteristics of the laminated plates have been evaluated. Furthermore, the possibility of utilizing SMA composite in applications where the event of an impact need to be considered is of fundamental importance to collect data on impact resistance of candidate materials and to predict the impact resistance. For this reason, the hybrid samples were tested in a Charpy geometry (Ref 11) using a hammer equipped with a piezoelectric sensor providing force-time and force-displacement curves during the impact test. Finally, a quasi-static analysis was performed, according to ASTM D790 (Ref 12), to evaluate the effect of hybridization on the static flexural properties of the laminates.

2. Materials and Methods

2.1 Materials

A SMA wire made of superelastic 56.00 wt.% Ni balance Ti alloy, straight annealed, and provided by SAES GETTERS was used. The superelastic wires are of 100 μm diameter in the straight configuration and 200 μm in the "zigzag shape" configuration. They include Austenite Finish temperature $A_f = -15$ °C as measured on finished wires, upper plateau stress (at 4% strain) $\cong 400$ MPa, and lower plateau stress (at 4% strain) $\cong 100$ MPa. Moreover, steel wires made of AISI 304L alloy with 100 μm diameter, 700 MPa break stress, and 5% break deformation, provided by COMAR S.r.l., were embedded in the straight configuration to make the comparison with equivalent SMA composites.

To embed SMA wires into the composite layers, special frames were designed to allow embedding the wires into the matrix equally spaced (with a distance between the wires equal to 1 mm) and aligned in the principal direction of the sample. Four layers of wires have been embedded in the composites at different distances from the neutral axis, near the external surfaces of the specimen. Instead, in the second configuration, special hybrid textile preforms (HEP) were realized by Extreme Materials, a company involved with the development of innovative hybrid textiles for technical uses. In these preforms, SMA wires are knitted within the fabric structure together with reinforcing glass bundles with a zigzag shape (patent pending). The volume percentage of metallic wires embedded into the two laminates is about the same and equal to 1%.

The laminates have been realized by vacuum-assisted resin infusion process. In the straight configuration, a vinylester resin Distitron VE370SC provided by Polynt was poured into a vacuum bag in which the frame necessary for the embedding of wires was positioned. Instead, in the second configuration, the wires are positioned by means of the textile preforms in which SMA wires are knitted with the glass fibers. These hybrid preforms have been laminated far from the neutral axis of the laminated to enhance the influence of SMA. So five different laminates have been realized and tested to evaluate the influence of hybridization:

– Traditional glass-reinforced laminates with SMA wires in a straight configuration by infusion of EE425 preforms (laminate 1);
– Hybrid glass-reinforced laminates with SMA wires in a straight configuration by infusion of EE425 preforms (laminate 1-SMA);
– Hybrid glass-reinforced laminates with steel wires in straight configuration by infusion of EE425 preforms (laminate 1-steel);
– Glass-reinforced laminates with HEP preforms (laminate 2-SMA); and
– Glass-reinforced laminates with Extreme Materials glass (EP) preforms (laminate 2).

The dimensions of the samples for damping characterization were 250×40 mm, whereas for impact and static flexural characterization the dimensions were 80×12.7 mm.

In Table 1, materials and stacking sequences of the composite laminates in which SMA and steel wires have been embedded are reported.
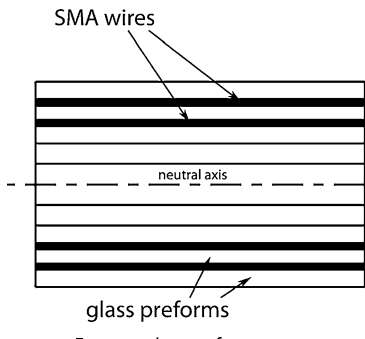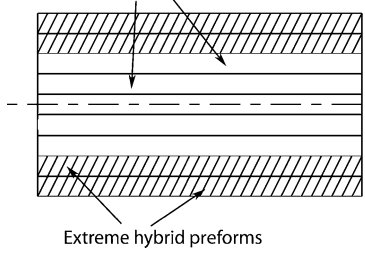
2.2 Experimental Methods

From the realized laminates, two types of specimens were obtained for damping and mechanical characterization: specimens without any metallic wires and hybrid specimens embedding SMA wires. Moreover, for the unidirectional configuration, specimens with embedded steel wires have also been fabricated. The wires have been embedded along the principal direction of the samples (see Fig. 1). In this figure, it is possible to see the predeformed regions of these wires in the knitted configuration.

2.2.1 Laser Vibrometry Measurement Setup. The schematic of the vibration testing setup is shown in Fig. 2. The samples (target) were clamped on one end by a vice and were excited in a controlled and repeatable manner by impacts with a pendulum. The active length of the samples was 212 mm and the impact point was positioned 110 mm from the free end. The release of the pendulum was controlled by an electromagnet. A Brüel & Kjaer type 4393 accelerometer with a mass of 5.6 g (including mount) and a sensitivity of 0.316 pC/(m/s^2) was attached to the pendulum to register the impact start. The impact velocity was 0.87 m/s.

The laser vibrometer system used is a Polytec PSV 300 scanning system. It is an interferometric device that uses a continuous wave He-Ne laser with a wavelength of 632.8 nm. The system measures the velocity of the vibrating target without contact.

The time responses of the composite plates were recorded after each impact. The sensitivity of the laser vibrometer was set to 10 mm/s/V with a range of 10 V. The measurements were trigged by the sharp slope of the accelerometer signal caused by the impact. Both signals were sampled at 1.28 kHz by the laser vibrometer system. The frequency response of each

Table 1 Materials and stacking sequences of the realized hybrid composites

SMA arrangements	Materials	Stacking sequences	Side views
Straight Laminate 1	SMA wires 100 μm provided by SAES Getters Steel wires 100 μm Glass Fabric EE425 Vinylester resin Distritron VE370SC by Polynt Thickness 3 mm	$[0°, W, 0°, W, (0°, 90°, 0°)]_S$	SMA wires ... neutral axis ... glass preforms
Knitted Laminate 2	SMA wires 200 μm Extreme hybrid preforms Extreme Materials' glass preforms Vinylester resin Distritron VE370SC by Polynt Thickness 4.2 mm	$[HEP, HEP, EP_2, \overline{EP}]_S$	Extreme glass preforms ... Extreme hybrid preforms

W indicates the metallic wires in the straight configuration, HEP indicates Hybrid Extreme Materials preforms, and EP indicates Extreme Materials preforms

measurement was calculated where natural frequencies and damping of each resonant mode were obtained.

2.2.2 Mechanical Characterization. Impact tests have been performed according to the Charpy test method (ASTM D256, Ref 11) by an instrumented impact tester. In Fig. 3, a schematization of sample geometry, positioning, and testing procedure is reported. The pendulum hammer was equipped with an ICP® Dynamic Force Sensor provided by PCB Piezoelectronics providing the force as a function of the time during the impact test. The impact height, H, was 0.74, while E was determined using $E = mgh$, where E is the energy, m is the mass of the impact head (equal to 3.48 kg), and g is the acceleration due to gravity. Non-notched samples of dimensions 12.7×80 mm were rested freely against two anvils and struck in the center by a pendulum. The results shown are an average between four and eight specimens of each type.

Static flexural tests have been performed by 3-point bend procedure (ASTM D790, Ref 12): the results are an average of 15 specimens of each type, and their dimensions were the same of Charpy tests.

2.3 Approach

2.3.1 Laser Vibrometry Analysis. Damping or loss factor measurements are rarely straightforward due to the complexity of the dynamic interaction of system joints, trim, and geometry (Ref 13-16). Furthermore, a variety of nomenclature exists to denote damping. These include: damping ratio (ζ), log decrement (δ), loss factor (η), loss angle (Φ), etc. Consequently, equal to the number of different descriptors for damping levels there are different test methods.

In this work, we have chosen to report the measure of the damping system by damping ratio values, and therefore how long the system will take to reach its final value. It is defined as the ratio of the damping constant to the critical damping constant:

$$\zeta = \frac{c}{c_c}$$

If the damping ratio is low, the system can oscillate for longer period (underdamping), whereas if it is high, it may not oscillate at all (overdamping). For this reason, an increase of damping ratio of the system leads to an enhancing of its damping properties and a reduction of the resonant effects.

A possible way to determine the amount of damping in a system is to measure the rate at which the oscillation decays. The logarithmic decrement method described in Ref 13 was used in this work to calculate the damping ratio.

In this experiment, not only the material and support causes damping but also the surrounding air. But, since the geometry and the eigenfrequencies are nearly the same for the samples (e.g., Laminate 1 or 2), the air damping will be the same.

2.4 Impact Analysis

In Fig. 4, a typical force-displacement curve resulting from a Charpy test on a composite sample is reported (Ref 17). The energy needed to break the sample is the area obtained integrating this curve. One method of expressing impact energy, for a plastic or a composite, is in terms of the formula: $U = E/bd$, where U is the impact energy, E is the energy registered in the test, b is the width of the specimen, and d is its thickness. Moreover, by integrating the area under the load-displacement curve and noting the value up to the maximum load or the load at first failure, it is possible to deduce the energy required to start or initiate damage and relate it to the energy of propagate damage. The ratio of the propagation energy E_p to the initiation energy E_i is known as the ductility
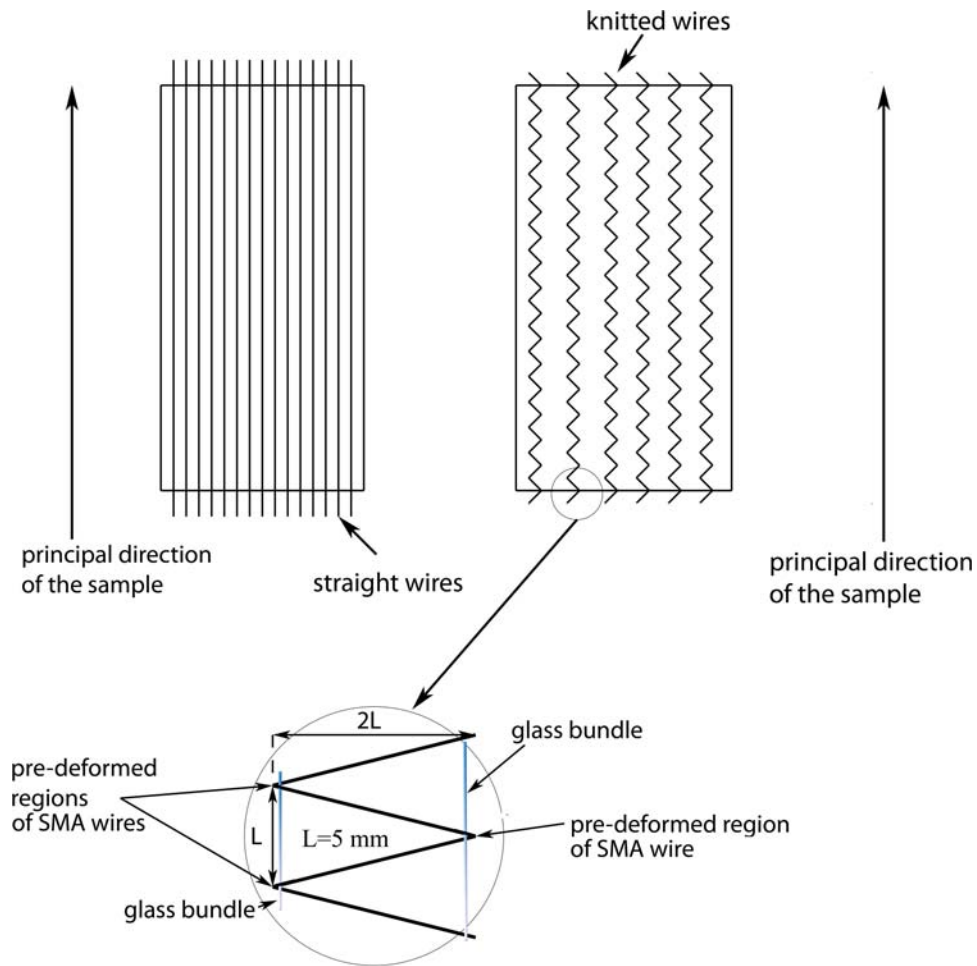
Fig. 1 Schematic diagram of the two configurations of the wires in the samples

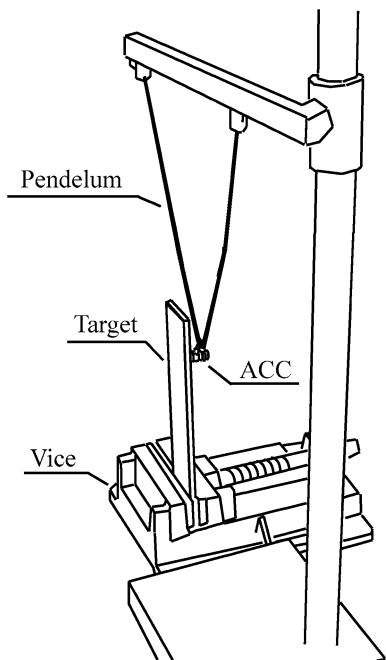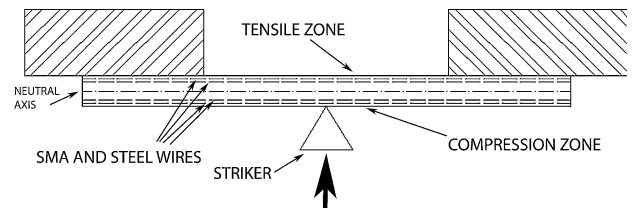**Fig. 2** The schematic of the vibration testing setup; ACC, accelerometer

Fig. 3 Schematization of sample geometry, positioning, and testing procedure

index D, which is calculated by the formula $D = E_p/E_i$. For these reasons, the ductility of the material is enhanced only if both U and D increase, otherwise if only U increases it can be considered as a brittle reinforcement of the material behaving like the other reinforcement.

3. Experimental Results

3.1 Laser Vibrometry Analysis

Figure 5 shows the calculated frequency responses of the laminate 1 sample obtained from laser vibrometry measurements. In Fig. 5(a), the first bending frequencies of the samples
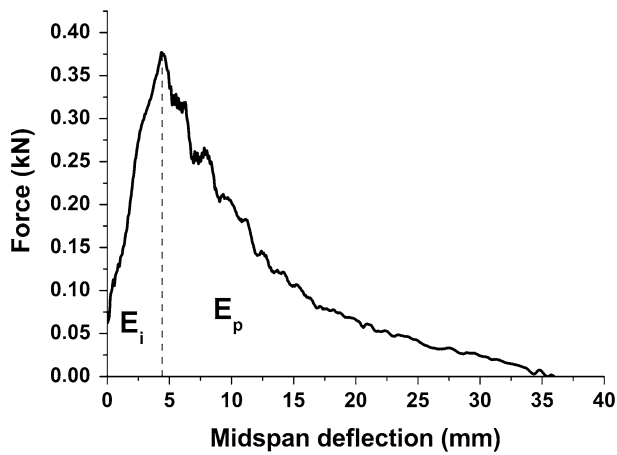
Fig. 4 Typical force-displacement curve resulting from a Charpy test on a composite sample

Fig. 5 (a) Plots of the first bending frequency response for the laminate 1 samples and (b) Plots of the second bending frequency response for the laminate 1 samples
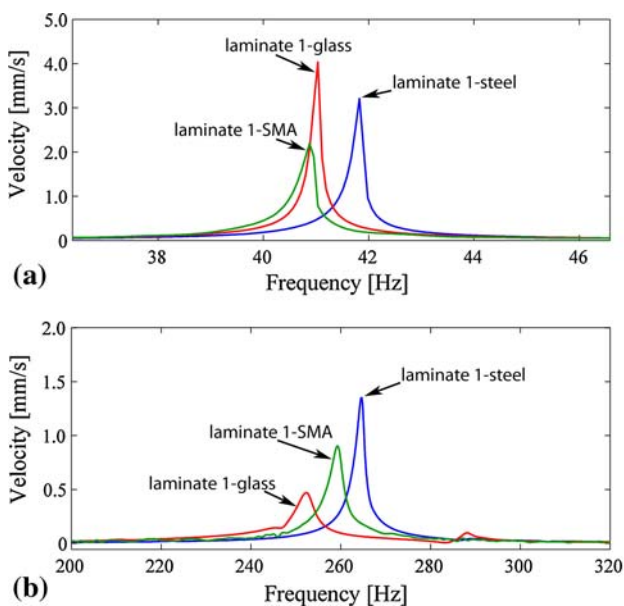

Fig. 6 (a) Plots of the first bending frequency response for the laminate 2 samples and (b) Plots of the second bending frequency response for the laminate 2 samples

are shown. Clearly, the SMA-fiber-reinforced composite has the smallest vibration velocity amplitude at this frequency. The damping ratios are: laminate 1-SMA ζ = 0.25%, laminate 1-steel ζ = 0.19%, and laminate 1-glass ζ = 0.18%. In Fig. 5(b), the second bending frequencies are shown. The corresponding damping ratios are: laminate 1-SMA ζ = 0.50%, laminate 1-steel ζ = 0.32%, and laminate 1-glass ζ = 0.73%. The laminate 1-glass sample has a small peak at 288 Hz which is its first torsional frequency.

So, embedding straight SMA wires into traditional composites has increased the damping ratio for the first bending ratio, while the influence of steel wires is lower. However, the positive effect provided by SMA wires cannot be related to the hysteresis loss which characterize these materials; in fact, the maximum strain at the beginning of vibration at the fixed end is about 50 microstrain, not big enough for the onset of the
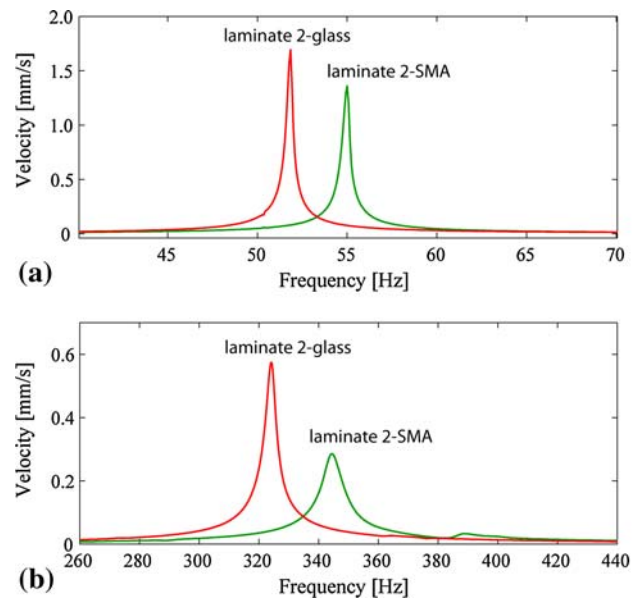
reverse martensitic transformation (that is about 10,000 microstrain). Moreover, for the second bending frequency, SMA hybridization causes a decrease of damping ratio (even if less considerable than for steel wires).

The calculated frequency responses of the laminate 2 samples obtained from laser vibrometry measurements are shown in Fig. 6. In Fig. 6(a), the first bending frequencies of the samples are shown. The natural frequency of the laminate 2-SMA sample is slightly higher compared to the laminate 2-glass sample. The damping ratios are also increased: laminate 2-SMA ζ = 0.32% and laminate 2-glass ζ = 0.29%. In Fig. 6(b), the second bending frequencies are shown, where the damping ratios are laminate 2-SMA ζ = 0.93% and laminate 2-glass ζ = 0.51%.

Clearly, the wrinkled SMA-fiber configuration induces a significant increase of the damping ratio for both the first and the second bending frequencies. In this case, this positive result is probably due to the initial deformation applied to the wires during knitting process. Further studies are necessary for concluding if this difference has a considerable effect in practical situation.

Finally, field measurements were obtained by scanning the laser beam across the surface where a grid of 36 points was measured. The mode shapes of the samples are shown in Fig. 7 where the lower ends are the fixed positions and the upper ends are the free ends. The color coding represents velocities, where the blue and the red areas are vibrating out of phase relative to each other. In Fig. 7(a), the first bending mode of the laminate 1-SMA sample is shown where the farther the fixed end the larger the velocities are. In Fig. 7(b), the second bending mode of the laminate 1-SMA sample is shown where the surface is split by a horizontal nodal line in the upper part of the sample. The first twisting mode of the laminate 1-glass sample is shown in Fig. 7(c) where the surface is split by a vertical nodal line. This mode is, however, only slightly generated since the impact point is positioned in the middle of cantilever.
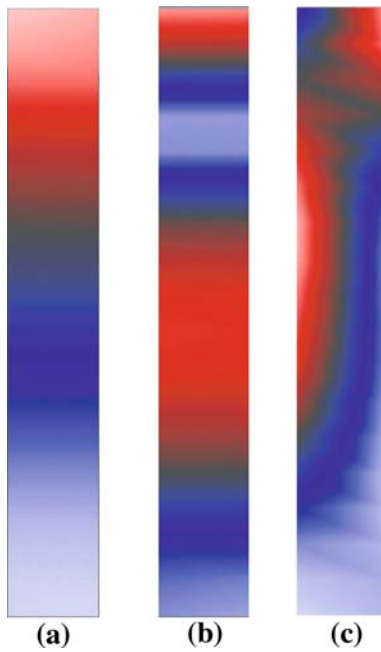
Fig. 7 Mode shapes of the laminate 1-samples: (a) laminate 1-SMA first bending mode, (b) laminate 1-SMA second bending mode, and (c) laminate 1-glass first twisting mode. Color coding: light blue, zero velocity and light red, maximum velocity

Table 2 Synthesis of Charpy test results

Laminate	E/A, J/mm^2			D		
	No wires	Steel wires	SMA wires	No wires	Steel wires	SMA wires
Laminate 1	0.215	0.205	0.211	1.14	1.37	1.47
		−4.7%	−1.86%		+20.2%	+28.9%
Laminate 2	0.112	···	0.153	1.03	···	1.19
			+36.6%			+15.5%

The increases are referred to the absorbed energy or D index of the samples without metallic wires

3.2 Impact Analysis

A synthesis of the Charpy and static flexural results is reported in Table 2 and 3. The average F/A (where F is the load measured during Charpy tests and A is the area of the cross section of the samples) and displacements impact curves for laminates 1 and 2 are shown in Fig. 8 and 9. The results are reported in terms of E/A (where E is the energy obtained by integrating the force-displacements curves) to take into account little increases of the thickness of the hybrid samples due to the introduction of the metallic wires.

As it is evident from tables and figures, SMA hybridization has a positive effect only for laminate 2, in which impact energy increases by +36.6%, compared with impact energy of the analogous nonhybrid samples. So, embedding SMA wires with the knitted configuration has increased the ductility of the laminate, as the increase of ductility index D (+15.5%) confirms. Instead, laminate 1 is only marginally affected by the hybridization, both for steel and SMA wires, since impact energy remains almost unchanged compared with analogous
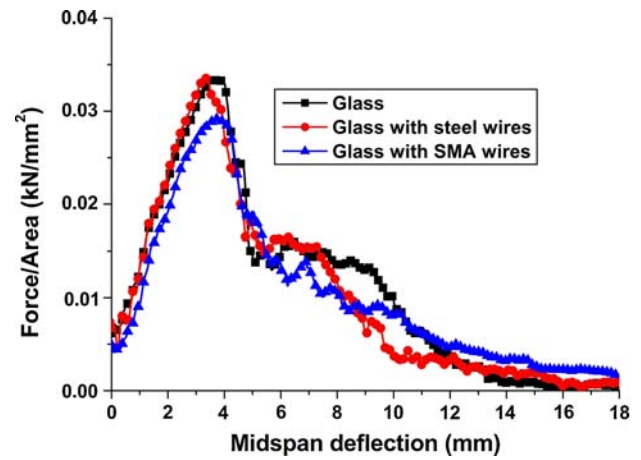

Fig. 8 Average force/area and displacements impact curves for laminate 1

Table 3 Synthesis of static flexural characterization results

	E_c, GPa	ε_r, %	σ_r, MPa
Laminate 1			
No wires	16.8	4.2	650
Steel wires	17.8	4.2	541
	+6%	···	−17%
SMA wires	15.5	4	513
	−8%	−5%	−21%
Laminate 2			
No wires	7.4	6.5	232.5
SMA wires	5.5	7.1	171
	−25.7%	+9.2%	−26.5%

The increases are referred to the absorbed energy of the samples without metallic wires
E_c, longitudinal flexural modulus, ε_r, longitudinal flexural strain, and σ_r, longitudinal flexural strength

nonhybrid sample. Moreover, the increase of D for hybrid laminate 1 (+28.9%) has to be related to the decrease of E_i caused by the decreases of the stiffness and ultimate loads of the laminate due to hybridization (see blue curve in Fig. 8).

This different influence of hybridization on the impact energy for the two laminates is probably due to the higher elastic modulus of laminate 1 which is twice the modulus of laminate 2. In fact, for laminate 1, the small amount of SMA wires (1% by volume) cannot influence the impact behavior of the composite. Moreover, laminate 1 has a higher break deformation, and so it is more ductile than laminate 2. On the other hand, laminate 2 presents lower modulus and lower deformation to break, which coupled with the knitted configuration of the embedded wires is probably responsible for the positive effect of hybridization. However, in both cases, hybridization causes a decrease of the static flexural properties that are affected by the external layers in each lay up configuration. Factors such as fiber crimping and fiber matrix adhesion can be responsible for the lower ultimate properties. For these reasons, tensile properties should be less affected by the presence of SMA wires.
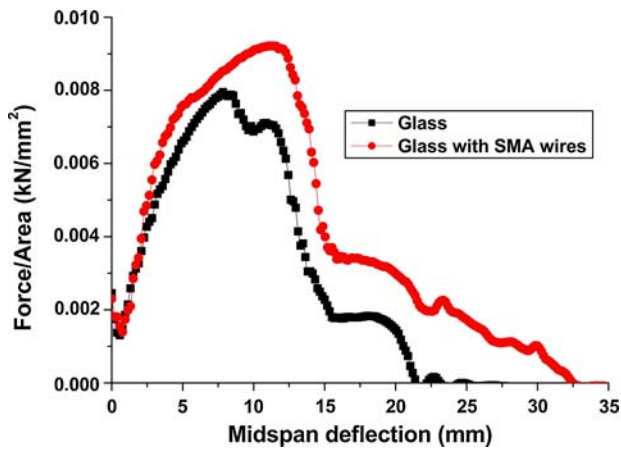
Fig. 9 Average force/area and displacements impact curves for laminate 2

4. Conclusions

In this work, the possibility of enhancing the damping properties of traditional glass-reinforced composites by means of SMA wires has been evaluated. Results show embedding SMA wires with a knitted configuration; thus, providing an initial deformation to the wires increases the positive effect of the hybridization. However, even with straight configuration there is an increase of the damping ratio for the first bending frequency, even if this effect cannot be related to the hysteretic behavior of superelastic alloys. Probably, this positive effect is due to the austenitic structure of SMA material in the laminate 1 and additionally to the martensitic structure of the predeformed regions in the knitted configuration. Further tests are needed to well investigate this phenomenon, for example, embedding SMA wires of smaller diameter with knitted configuration or embedding SMA predeformed wires in the straight configuration. Instead, it is clear that steel wires cannot increase damping properties of the composite.

Then, impact properties of hybrid composites indicated that SMA wires in the knitted configuration cause a considerable increase of impact strength, while a decrease of flexural mechanical properties due to hybridization was observed.

References

1. R. Stalmans, V. Michaud, J. E. Bidaux, R. Gotthardt, and J. A. E. Manson, Adaptive Composites with Embedded Shape Memory Alloy Wires, in *Proceedings of the 4th European Conference on Smart Structures and Materials*, G. R. Tomlinsonen and W. A. Bullough, Eds., Institute of Physics Publishing, Bristol, England, 1998, p 801–804

2. C. Boller, Shape Memory Alloys – Their Challenge to Contribute to Smart Structures, *Annual Meeting of the Materials Research Society*, Boston, MA (Invited paper)

3. R. Stalmans, Invited Lecture—Adaptive Hybrid Composites with a Focus on the Integration of Shape Memory Elements, *Adv. Sci. Technol.*, 1999, **25**, p 83–94, *Smart Materials Systems*, P. Vincenzini, Ed., June 14–19, 1998 (Florence, Italy), Techna, Faenza, Italy

4. R. Stalmans, K. Tsoi, and J. Schrooten, The Transformational Behaviour of Shape Memory Wires Embedded in a Composite Matrix, *Proceedings of SPIE Fifth European Conference on Smart Structures and Materials*, P. F. Gobin and C. M. Friend, Eds., May 22-25, 2000 (Glasgow, Scotland), 2000, **4073**, p 88–96

5. K. Tsoi, et al., Impact Damage Behavior of Shape Memory Alloy Composites, *Mater. Sci. Eng.*, 2003, **342**(1–2), p 207–215

6. K.-T. Lau, et al., Low Velocity Impacts on Shape Memory Alloy Stitched Composite Plates, *Smart Mater. Struct.*, 2004, **13**, p 364–370

7. R.-X. Zhang, and Q.-Q. Ni, et al., Vibration Characteristics of Laminated Composite Plates with Embedded Shape Memory Alloy, *Compos. Struct.*, 2006, **74**, p 389–398

8. Q.-Q. Ni, and R.-X. Zhang, et al., Stiffness and Vibration Characteristics of SMA/ER3 Composites with Shape Memory Alloy Short Fibers, *Compos. Struct.*, 2007, **79**, p 501–507

9. W. M. Ostachowicz, and S. Kaczmrczyk, Vibration of Composite Plates with SMA Fibers in a Gas Stream with Defects of the Type of Delamination, *Compos. Struct.*, 2001, **54**, p 305–311

10. T. L. Turner, Structural Acoustic Response of a Shape Memory Alloy Hybrid Composite Panel, *Proc. SPIE*, 2002, **4701**, p 592–603

11. ASTM D256-04, *Standard Test Methods for Determining the Izod Pendulum Impact Resistance of Plastics*, ASTM International, 2004, p 1–20

12. ASTM D790-03 *Standard Test Methods for Flexural Properties of Unreinforced and Reinforced Plastics and Electrical Insulating Materials*, ASTM International, 2003, p 1–11

13. D.J. Inman, *Engineering Vibration*, 3rd ed., Prentice-Hall International Editions, Upper Saddle River, NJ, 2008

14. W.T. Thomson and M. D. Dahleh, *Theory of Vibration with Applications*, 5th ed., Prentice-Hall, Upper Saddle River, NJ, 1998

15. A.A. Shabana, "Theory of Vibration," Drugaizdaja, University of Illinois, Chicago, 1995

16. L.E. Drain, 1980, *The Laser Doppler Technique*, Wiley, London

17. S.R. Reid and G. Zhou, *Impact Behaviour of Fibre-Reinforced Composite Materials and Structures*, Woodhead Publishing Ltd., Cambridge, UK, 2000